# Dynamics of trapped charge in GaN/AlGaN/GaN high electron mobility transistors grown by plasma-assisted molecular beam epitaxy

Oleg Mitrofanov and Michael Manfra

Citation: Appl. Phys. Lett. **84**, 422 (2004); doi: 10.1063/1.1638878
View online: http://dx.doi.org/10.1063/1.1638878
View Table of Contents: http://apl.aip.org/resource/1/APPLAB/v84/i3
Published by the American Institute of Physics.

# Dynamics of trapped charge in GaN/AlGaN/GaN high electron mobility transistors grown by plasma-assisted molecular beam epitaxy

Oleg Mitrofanov[a] and Michael Manfra
*Bell Laboratories, Lucent Technologies, 600 Mountain Avenue, Murray Hill, New Jersey 07974*

(Received 9 September 2003; accepted 12 November 2003)

We report on the dynamics of trapped charge in unpassivated GaN/AlGaN/GaN high electron mobility transistors grown by plasma-assisted molecular beam epitaxy. Trap states are probed using a transient channel-current technique. By tailoring the gate pulse depth and width, this method allows selective probing of different trapping centers. We have identified at least two different trap centers that influence the current dynamics in our structures. In addition, the charge emission from the faster trap is found to have a clear square-root dependence on the applied electric field. This unambiguous field dependence allows us to isolate the mechanisms responsible for emission. We also identify the trapping mechanism and estimate the characteristic time required to fill available trap states and a lower bound for the trap density. © *2004 American Institute of Physics.*
[DOI: 10.1063/1.1638878]

Trapping effects in AlGaN/GaN high electron mobility transistors (HEMTs) currently present a major limitation on the power performance at high frequencies.[1] Parasitic charge trapped on the surface and/or in the bulk of the heterostructure alters the density of the two-dimensional electron gas (2DEG) in the channel and limits switching characteristics of the device. Considerable research effort has been directed toward identification and elimination of the trapping effects in AlGaN/GaN transistors.[2–7] However, the majority of the studies have been limited to qualitative description. The trap states, their activation energies, and the physical mechanisms responsible for capture and emission are far from understood in any quantitative manner. Identifying the spatial and energetic location of the traps and the mechanisms by which charge moves in and out of the trapping centers, is essential for understanding and eliminating the effects of the traps on the device performance. Recently, we reported on trapping behavior in molecular beam epitaxy (MBE) grown unpassivated GaN/AlGaN/GaN HEMTs.[8] The observed effects indicated that electrons are trapped when a negative voltage is applied to the gate. It was noted that several traps might influence the current dynamics.

In this letter, we report on the dynamics of the trapped charge measured by a more elaborate transient channel-current technique. By tailoring the gate pulse depth and width, this method allows selective probing of different trapping centers. We have isolated at least two different traps that influence the current dynamics in our structures. In addition, the rate of charge emission from the traps is found to have a clear square-root dependence on the applied electric field. This unambiguous field dependence allows us to deduce the mechanisms responsible for emission. We also identify the trapping mechanism and estimate the characteristic time required to fill available trap states and a lower bound for the trap density.

This study is performed on *undoped* GaN/AlGaN/GaN HEMTs grown by plasma-assisted MBE on semi-insulating SiC substrates. Undoped structures are chosen because larger trapping effects are observed as compared to structures with Si doping in the barrier.[8] The structure consists of an approximately 2-$\mu$m-thick GaN buffer layer, a 30-nm-thick $Al_{0.34}Ga_{0.66}N$ barrier, and a 5-nm-thick GaN capping layer. Typical room temperature 2DEG mobilities are $\sim 1400\ cm^2/V\,s$ at a sheet density of $1.2\times10^{13}\ cm^{-2}$. The devices have source–drain and gate–drain openings of 5 and 2 $\mu$m, respectively. The gate length is 1 $\mu$m and the width is 100 $\mu$m. The device surface is not passivated.[8–11]

The occupation factor of the traps is defined by the capture and emission processes, which balance each other in the steady state. Under the applied negative gate bias, electrons from the gate electrode can tunnel through the metal–semiconductor interface. The electrons can be temporally trapped, resulting in an increase of the occupation factor. When the gate voltage is turned off, the system of trapped electrons finds itself far from equilibrium. With the trap filling mechanism interrupted, the emission process alone determines the dynamics of the trap population until the equilibrium is reached. If the trapping center is characterized by a localized level in the band gap, the nonequilibrium population of the traps decreases exponentially with time.

The dynamics of the trapped charge is reflected in the transistor drain current. In the experiment, the device is continuously held at a constant source–drain bias $V_D$ in the common source configuration, resulting in a steady state channel current $I_D^{SS}$. To fill the trap states, the gate voltage is switched from the high level $V_G^{SS}=0$ V to the low level $V_G^{Pulse}$ for a short period of time $t_p$. The drain current drops in the response to the gate pulse. As the gate potential is switched to the initial level, the drain current recovers only to a level $I_D^{SS}-\Delta I_D$, from which the current gradually approaches the steady state value. This approach corresponds to the emission of the trapped charge. The drain current transient is measured using a low insertion impedance current probe. The emission rate is deduced by fitting the current change $\Delta I_D(t)$ with an exponential decay function.

[a]Electronic mail: olegm@lucent.com

 

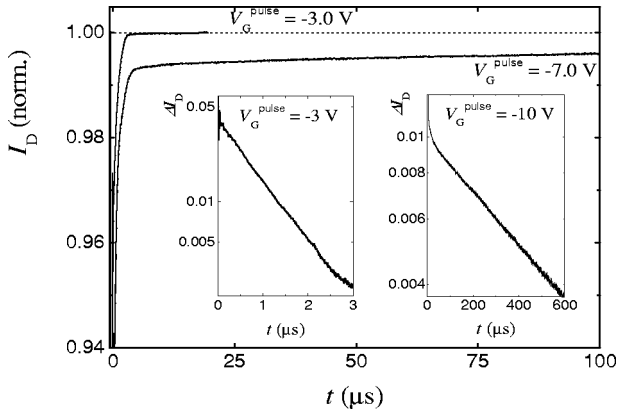


FIG. 1. Channel-current transients after 500 ns gate filling pulses. The current is normalized to the steady state value. The source–drain voltage $V_D = 6$ V. Insets show the difference between the steady state and the transient current for the shallow ($V_G^{\text{Pulse}} = -3$ V) and deep ($V_G^{\text{Pulse}} = -10$ V) filling pulses.

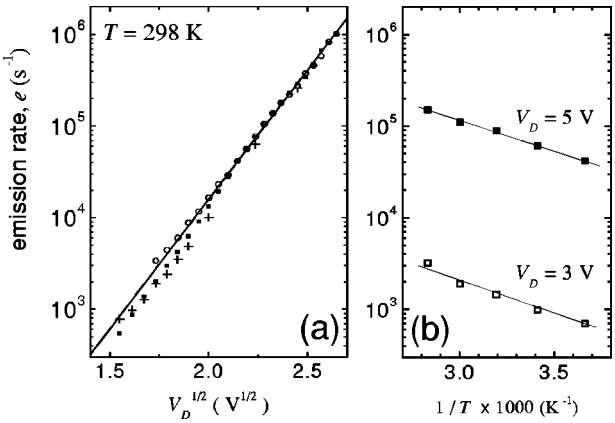


FIG. 2. (a) Emission rate extracted from the fast transient as a function of the drain–gate potential difference during the emission process ($V_G = 0$ V). Nonequilibrium trap occupation is created by a 350 ns gate pulse $V_G^{\text{Pulse}} = -3$ V. (b) Emission rate as a function of temperature for two gate–drain biases: $V_D = 3$ V and $V_D = 5$ V.

A typical response of the channel current to a short (500 ns) filling gate pulse reflects at least two charge emission processes. Figure 1 shows the current transient where both processes are clearly seen ($V_G^{\text{SS}} = 0$ V, $V_G^{\text{pulse}} = -7$ V, $V_D = 6$ V). Recovery of the channel current after the filling pulse starts with a fast transient. After few microseconds, as the current level reaches ~99% of the steady state level, the dynamics slows down. The amplitude of the fast transient is larger and it is dominant within the first microseconds. The slower dynamics becomes dominant later and lasts for hundreds of microseconds. For shallow filling pulses, the amplitude of the slow transient is, typically, negligible. The inset of Fig. 1 shows the difference current $\Delta I(t)$ normalized to the saturation value $I_D^{\text{SS}}$ for $V_G^{\text{pulse}} = -3$ V. The trap occupation decreases exponentially with the characteristic time of ~1 $\mu$s. The slower process can be measured using deeper filling pulses. Inset 2 shows $\Delta I(t)$ for $V_G^{\text{pulse}} = -10$ V. The characteristic time of this process is larger by two orders of magnitude and the amplitude of the transient is substantially smaller. The emission transients are clearly related to two different trapping centers.

In order to better understand the emission mechanism we focus our study on the faster process. Interestingly, the faster emission process exhibits a strong dependence on the external electric field that exists in the region of the trapped charge due to the potential difference between the gate and the drain. The characteristic emission time rapidly increases from a few milliseconds at low fields ($V_D = 2.5$ V) to submicrosecond at higher fields ($V_D = 7-8$ V). To determine the functional dependence, the measured values of the emission rate are fitted with a power-law function ($\ln e = a + bV^p$). The result of the fitting suggests that the emission rate increases exponentially with the square root of the applied field ($p = 0.53$). Figure 2(a) shows the emission rate plotted versus the square root of the drain voltage $V_D$ for three separate devices. The solid line shows a fit to the data $e = \exp[a + b\sqrt{V_D}]$, where $a = -3.3 \pm 0.2$ and $b = 6.5 \pm 0.4$ $V^{-1/2}$.

The functional dependence of the emission rate suggests the Poole–Frenkel (PF) mechanism of charge emission.[12] The barrier height of the trap in the presence of electric field $\mathcal{E}$ becomes field dependent $\phi(\mathcal{E}) = \phi(0) - \sqrt{q^3\mathcal{E}/\pi\varepsilon}$ (for a Coulombic center), where $\phi(0) = E_T$ is the binding energy of the electron in the zero field and $q$ and $\varepsilon$ are the electron charge and the dielectric constant. The probability of the thermal emission increases exponentially with the square root of the field: $\ln e(\mathcal{E}) \propto \sqrt{\mathcal{E}}$.

One implication of the PF effect is that the activation energy of the emission process, which equals the trap barrier height, decreases with the applied field. The drop of the potential barrier due to the PF effect can be extracted from the ratio of the emission rates at different applied fields: $\Delta\phi = kT \ln[e(\mathcal{E}_1)/e(\mathcal{E}_2)]$. For example, for the source–drain voltage increase from 3 to 5 V, the increase in the emission rate corresponds to the potential barrier drop of $0.09 \pm 0.01$ eV.

The emission rate as a function of the inverse temperature is shown in Fig. 2(b) for two source–drain voltages $V_D = 3$ V and $V_D = 5$ V in the temperature range of 273–353 K. Fitting the data with the function $e = AT^2 \exp(-E_A/kT)$ results in apparent activation energies of $0.10 \pm 0.02$ and $0.08 \pm 0.01$ eV a for $V_D = 3$ V and $V_D = 5$ V, respectively. The data demonstrate a small decrease in activation energy at higher electric fields expected from the PF effect, however, the error bars are large. At this point, we cannot rule out the presence of competing emission mechanisms.

The width and the depth of the filling pulse have practically no effect on the emission *rate*, however, the *amplitude* of the transient critically depends on the filling pulse parameters. As the negative gate bias is applied, the electrons start tunneling through the Schottky barrier and filling the available trapping sites. The number of occupied traps increases with time until it reaches the equilibrium and the capture and emission processes balance each other. This behavior is reflected in the amplitude of the transient current $\Delta I(t = 0)$, shown in Fig. 3(a) as a function of the filling pulse width. The characteristic time required to fill the available states is on the order of 5–10 $\mu$s.

The number of the occupied traps also increases with the depth of the filling pulse [Fig. 3(b)]. Efficient filling of the trap states starts only for deep gate pulses, when a large electric field substantially tilts the bands in the barrier. The field increases the probability for electrons to tunnel from the

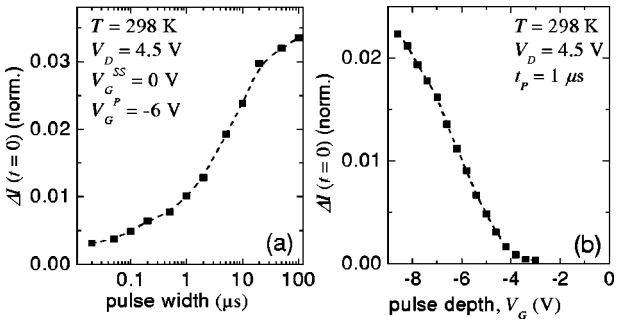


FIG. 3. Amplitude of the current transient as a function the width (a) and depth (b) of the filling gate pulse.

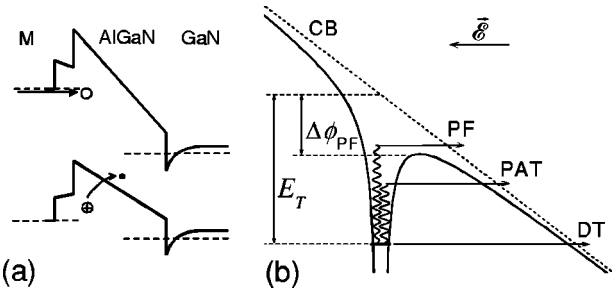


FIG. 4. (a) Schematic diagram of the capture (top) and the emission (bottom) processes in GaN/AlGaN/GaN HEMTs. (b) Three possible mechanisms of emission from the trap in the presence of the electric field: Poole-Frenkel emission (PF), phonon-assisted tunneling (PAT), and direct tunneling (DT).

gate into the semiconductor. For even deeper gate pulses the amount of the trapped charge saturates. Characteristics similar to ones shown in Fig. 3 were obtained for temperatures $T=200$ and 100 K, indicating that the capture process is not thermally activated.

To estimate the density of the occupied traps, we establish a relationship between the change of the channel current and the amount of the trapped charge $Q_T$. It follows from PF effect data that the active trapping centers are confined to the region of very high electric field ($>0.5$ MV/cm at $V_{GD}=5$ V). The centers therefore can be located only in the vicinity of the gate edge, either in the barrier or on the open surface where the fringing field is strong. The GaN/AlGaN/GaN heterostructure transistor can be considered as a parallel plate capacitor with the gate as one electrode and the 2DEG as the other. Charge trapped in the barrier induces additional charge at the electrodes. The total amount of the induced charge equals the trapped charge and the distribution between the gate electrode and the 2DEG depends on the location of the trapped charge. The induced charge in the channel follows a simple expression:

$$\Delta q_{2\mathrm{DEG}} = -Q_T\left(1-\frac{d_{2\mathrm{DEG}}}{d}\right),$$

where $d$ and $d_{2\mathrm{DEG}}$ are the barrier thickness and the distance between the trapped charge and the channel. If the charge is trapped on the open surface, the amount of the induced charge in the channel equals the trapped charge $\Delta q_{2\mathrm{DEG}}=-Q_T$. In both cases the difference between the steady state current and the transient current $\Delta I(t)=I_D^{\mathrm{SS}}-I_D(t)$ is directly proportional to $Q_T$. A lower bound for the active trap density can be estimated from the saturation levels in Fig. 3. The 2DEG density in the steady state is $n\cong 10^{13}$ cm$^{-2}$ ($V_G=0$ V). Therefore a 2.5% change in the channel current corresponds to $Q_T \geqslant 2.5\times 10^{11}$ cm$^{-2}$.

The trapping process in our GaN/AlGaN/GaN HEMTs can be illustrated in Fig. 4. The top diagram of Fig. 4(a) shows the HEMT structure under the applied gate filling pulse. Electrons tunnel into the trap states through the Schottky barrier. After the gate voltage is removed, the electrons start slowly escaping from the traps (bottom diagram). The three competing emission processes are illustrated in Fig. 4(b). The efficiency of each process depends on the temperature, applied field, and the binding energy of an electron on the trap.

In conclusion, we report on the study of the trapping effects in unpassivated GaN/AlGaN/GaN HEMTs by a transient channel-current technique. By tailoring the width and depth of the filling gate pulse two different traps can be activated. Electrons are trapped on the fast states via tunneling from the gate within 5–10 $\mu$s after applying a negative gate bias. The emission rate from the faster traps is found to increase exponentially with the square root of the electric field due to the trap potential barrier lowering (PF effect). The emission process at room temperature is dominated by thermal ionization, however, other mechanisms cannot be excluded, particularly at high bias conditions. A lower bound for the trap density is about $10^{11}$ cm$^{-2}$.

The authors wish to acknowledge J. W. P. Hsu and D. V. Lang for useful discussions.

[1] S. C. Binari, P. B. Klein, and T. E. Kaizor, Proc. IEEE **90**, 1048 (2002).
[2] B. M. Green, K. K. Chu, E. M. Chumbes, J. A. Smart, J. R. Shealy, and L. F. Eastman, IEEE Electron Device Lett. **21**, 268 (2000).
[3] R. Vetury, Q. Zhang, S. Keller, and U. K. Mishra, IEEE Trans. Electron Devices **48**, 560 (2001).
[4] S. C. Binari, K. Ikossi, J. R. Roussos, W. Kruppa, D. Park, H. Dietrich, D. D. Koleske, A. E. Wickenden, and R. L. Henry, IEEE Trans. Electron Devices **48**, 565 (2001).
[5] A. V. Vertiatchikh, L. F. Eastman, W. J. Schaff, and T. Prunty, Electron. Lett. **38**, 388 (2002).
[6] A. Tarakji, G. Simin, N. Ilinskaya, X. Hu, A. Kumar, A. Koudymov, J. Yang, M. A. Khan, M. S. Shur, and R. Gaska, Appl. Phys. Lett. **78**, 2169 (2001).
[7] I. Daumiller, D. Theron, C. Gaquiere, A. Vescan, R. Dietrich, A. Wieszt, H. Leier, R. Vetury, U. K. Mishra, I. P. Smorchkova, S. Keller, N. X. Nguyen, C. Nguyen, and E. Kohn, IEEE Electron Device Lett. **22**, 62 (2001).
[8] O. Mitrofanov, M. Manfra, and N. Weimann, Appl. Phys. Lett. **82**, 4361 (2003).
[9] N. G. Weimann, M. J. Manfra, S. Chakraborty, and D. M. Tennant, IEEE Electron Device Lett. **23**, 691 (2002).
[10] M. J. Manfra, N. Weimann, Y. Baeyens, P. Roux, and D. M. Tennant, Electron. Lett. **39**, 694 (2003).
[11] N. G. Weimann, M. J. Manfra, and T. Wachtler, IEEE Electron Device Lett. **24**, 57 (2003).
[12] J. G. Simmons, Phys. Rev. **155**, 657 (1967).